International Immunopharmacology 75 (2019) 105759

Contents lists available at ScienceDirect

International Immunopharmacology

journal homepage: www.elsevier.com/locate/intimp

# Methyl helicterilate ameliorates alcohol-induced hepatic fibrosis by modulating TGF-β1/Smads pathway and mitochondria-dependent pathway

Shujuan Wen[1], Yuanyuan Wei[1], Xiaolin Zhang, Facheng Bai, Shimei Tan, Jinlan Nie, Jinbin Wei*, Xing Lin*

*Guangxi Medical University, Nanning 530021, China*

ARTICLE INFO

*Keywords:*
Methyl helicterilate
*Helicteres angustifolia*
Alcohol
Hepatic fibrosis
Hepatic stellate cells
TGF-β1/Smads pathway

ABSTRACT

This study aimed to investigate the effect and underlying mechanism of Methyl helicterilate from *Helicteres angustifolia* (MHHA) on alcohol-induced hepatic fibrosis. The results showed that MHHA treatment markedly alleviated alcohol-induced liver injury and notably reduced collagen deposition in liver tissue. It significantly enhanced the activity of alcohol dehydrogenase and aldehyde dehydrogenase. Moreover, MHHA treatment markedly decreased the content of inflammatory cytokines, alleviated collagen accumulation, and inhibited the expression of TGF-β1 and Smad2/3 in liver tissue. The experiments in cells showed that MHHA significantly inhibited HSC activation by blocking TGF-β1/Smads signaling pathway. Additionally, it notably induced HSC apoptosis by modulating the mitochondria-dependent pathway. The present study demonstrates that MHHA treatment significantly ameliorates alcoholic hepatic fibrosis and the underlying mechanism may be ascribed to the inhibition of the TGF-β1/Smads pathway and regulation of the mitochondria-mediated apoptotic pathway.

## 1. Introduction

Liver fibrosis is a pathologic process of chronic liver injury caused by various risk factors, which is characterized by the excessive deposition of extracellular matrix (ECM) [1]. Alcohol abuse is one of the major causes of liver fibrosis. Chronic alcohol ingestion is associated with defective gut motility, resulting in elevated endotoxin (lipopolysaccharide, LPS) in the liver. Interaction of LPS with Kupffer cell surface receptors elicits reactive oxygen species (ROS) production and cytokines release. Besides, the major metabolic product of alcohol, acetaldehyde also activates hepatic stellate cells (HSCs) that in turn triggers inflammatory and fibrogenic signals [2]. HSCs are the main fibrogenic cell type in the injured liver. Activated HSCs can produce the main components of ECM, directly participating in the progress of liver fibrosis [3]. Increasing evidence has indicated that transforming growth factor beta 1 (TGF-β1) and its downstream Smads strongly stimulate HSC activation, promoting collagen accumulation and fibrogenesis [4]. Activated TGF-β1 binding to the TGF-β type II receptor (TβRII) recruits the TGF-β type I receptor (TβRI), leading to the formation of the compound TGF-β1/TβRII/TβRI. Subsequently, Smad2 and Smad3 become phosphorylated and form heteromeric complexes with Smad4. After that, these activated Smad complexes translocate to the nucleus, where they can regulate the expression of the profibrotic genes [5]. Therefore, inhibiting HSC activation by blocking the TGF-β1/Smads pathway may be a potential target for the treatment of liver fibrosis [6].

Many natural compounds have been shown to have hepatoprotective effects. *Helicteres angustifolia* (Sterculiaceae) is a traditional herbal medicine in China, which has been used for the treatment of immune disorders and liver diseases [7]. In our previous studies, many natural compounds were isolated from *Helicteres angustifolia* and one of them was identified as methyl helicterilate (MHHA). In this study, we examined the effect of MHHA on alcohol-induced liver fibrosis in vivo and human hepatic stellate cells (LX-2) in vitro. The results showed that MHHA alleviated alcohol-induced liver fibrosis by inhibiting the TGF-β/Smads pathway. Furthermore, we also noticed that MHHA prevented fibrosis via regulating the mitochondria-mediated apoptotic pathway in HSCs. This study preliminarily demonstrates that MHHA is likely to be a potential natural medicine for the treatment of alcohol-induced liver fibrosis.

* Corresponding authors at: Guangxi Medical University, Nanning, Guangxi 530021, China.
*E-mail addresses:* jbwei@sina.cn (J. Wei), gxlx60@163.com (X. Lin).
[1] Shujuan Wen and Yuanyuan Wei contributed equally to this work.

https://doi.org/10.1016/j.intimp.2019.105759
Received 17 April 2019; Received in revised form 4 July 2019; Accepted 12 July 2019
Available online 17 July 2019

## 2. Materials and methods

### 2.1. Materials

*Helicteres angustifolia* was purchased from Nanning Qianjinzi Chinese Pharmaceutical Co. Ltd. (Nanning, China), which was identified by Professor Huang QF in the First Affiliated Hospital of Guangxi Traditional Chinese Medicine University. The specimen (LXHA120180325) was deposited in the Department of Pharmacology of Guangxi Medical University. Fetal bovine serum was purchased from Life Sciences (Grand Island, NY). Dimethyl sulfoxide (DMSO) and 3-(4, 5-dimethylthiazol-2-yl)-2, 5-diphenyltetrazolium bromide (MTT) were purchased from Sigma (USA). Alcohol dehydrogenase (ADH) and aldehyde dehydrogenase (ALDH) kits were purchased from Wuhan Boster Bio-Engineering Ltd. (Wuhan, China). Alanine transaminase (ALT) and aspartate transaminase (AST) kits were purchased from Nanjing Jiancheng Bioengineering Research Institute (Nanjing, China). TNF-α, IL-6 and IL-1β ELISA kits were purchased from Wuhan Boster Bio-engineering Co., Ltd., (Wuhan, China). Hyaluronic acid (HA), type III precollagen (PCIII), laminin (LN) and hydroxyproline (HYP) commercially available kits were purchased from Beijing Furui Bioengineering Research Company (Beijing, China). The antibodies including Col—I, Col-III, α-SMA, Bcl-2, Bax, cytochrome C, TGF-β1, p-Smad2/3, Smad2/3 and GAPDH were purchased from Santa Cruz Biotechnology (Santa Cruz, CA).

### 2.2. Preparation of MHHA

The dried root of *Helicteres angustifolia* (5 kg) was smashed and subject to sifting (40 mesh). The coarse powder was extracted by 95% ethanol reflux at 80 °C for three times (2 h per time). The solvent was evaporated under a vacuum. The crude extract was resuspended in water, and extracted with water-saturated n-butanol and ethyl acetate successively. The solvent was evaporated under a vacuum and the extract was then subjected to chromatography on a silica gel column (200–300 mesh, Yantai, PR China; Ø10 cm × 300 cm) eluting with a mixture of n-hexane, ethyl acetate, methyl alcohol and water (9: 1: 5: 5; 1500 mL each fraction). The third fraction yielded a white extract after concentration, which was further purified by chromatography on a silica gel column eluting with a mixture of n-hexane, ethyl acetate and methyl alcohol (9: 1: 8; 1500 mL each fraction). The second fraction yielded a colorless crystal (11.63 mg) after recovering the solvent. Its structure was elucidated on the basis of physicochemical properties and spectral data:

mp 152 °C. IR $\nu_{max}^{KBr}$: $cm^{-1}$ 1720, 1660, 1600, 1580, 1382, 1362, 1325, 1302, 1240, 1262. ESI-MS *m/z*: 632 $[M + H]^+$. $^1H$ NMR (300 MHz, $CDCl_3$) *δ*: 7.99 (2H, d, *J* = 7.5 Hz, H-2′, 6′), 7.58 (1H, td, *J* = 7.2 Hz, H-4′), 7.46 (2H, m, *J* = 7.6 Hz, H-3′, 5′), 5.66, 4.45 (1H, t, d, *J* = 3.1 Hz, H-12), 4.25 (1H, d, *J* = 12.9 Hz, H-27), 4.38 (1H, br s, *J* = 8.4 Hz, H-3α), 3.66 (3H, 17-$COOCH_3$), 2.93 (1H, dd, *J* = 4.1, 4.5 Hz, H-18), 2.02 (3H, s, 3-$OCOCH_3$), 0.96 (3H, s, H-25), 0.89 (3H, s, H-30), 0.85 (3H, s, H-24), 0.83 (3H, s, H-29), 0.77 (3H, s, H-23), 0.75 (3H, s, H-26). The results suggested that the compound is 3β-aeetoxy-27-benzoyloxy-olean-12-en-28-oie acid methyl ester, i.e., methyl helicterilate. Its molecular formula is $C_{40}H_{56}O_6$ and its chemical structure is shown in Fig. 1.

### 2.3. Animals and treatments

Male Wistar rats (SPF, 180 ± 10 g) were purchased from the Guangxi Medical University Experimental Animal Center (Guangxi, China) and the animal experiment was approved by the Guangxi Medical University Institutional Animal Care and Use Committee.

The treatment schedule was shown in Fig. 2. The rats were allowed to acclimate for one week and then divided into 6 groups (12 rats/group) including the normal group, MHHA control group (66.90 mg/kg MHHA), model group, and low-, middle- and high-dosages of MHHA-treated groups (16.72, 33.45 and 66.90 mg/kg MHHA). The animals in the MHHA control and MHHA -treated groups were orally administrated with MHHA for 24 weeks; the rats in the normal and model groups were received an equivalent volume of saline. Meanwhile, the animals in the model control and MHHA-treated groups were given intragastric edible alcohol with a gradually increased dose as previously described [8,9]: 5.0 g/kg/day from 1 to 4 weeks; 7.0 g/kg/day from 5 to 8 weeks; 9.0 g/kg/day from 9 to 12 weeks; and 9.5 g/kg/day from 13 to 24 weeks.

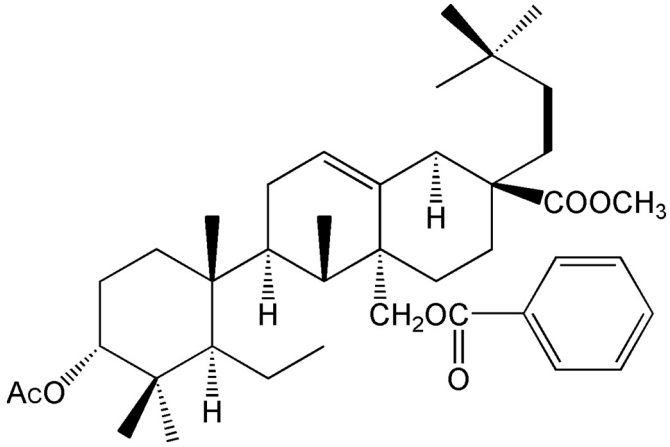


**Fig. 1.** The chemical structure of methyl helicterilate.

Four hours after the last treatment, the rats were intraperitoneally injected with ketamine hydrochloride (30 mg/kg). Blood samples were drawn from an abdominal artery and collected into heparinized tubes (50 U/mL). Liver of each rat was dissected out, washed with saline, and then divided into two parts; that is, one part was immediately stored at −80 °C for future analysis, and another was excised and fixed in 10% formalin solution for histopathologic examination.

### 2.4. Determination of metabolic enzymes activity

ADH and ALDH activity was measured using commercially available diagnostic kits (Wuhan Boster Bio-Engineering Ltd., Wuhan, China) according to the manufacturer's instructions. Moreover, the microsomal fraction of liver was prepared, and cytochrome P4502E1 (CYP2E1) was determined as previously described [10].

### 2.5. Pathological examination and immunohistochemical analysis

The fresh liver was dissected and fixed in 10% phosphate-buffered formalin, embedded in paraffin blocks. Around 5-micrometer-thick paraffin slices were sectioned and then respectively stained with Hematoxylin & Eosin (H&E), Masson's trichrome and Sirius red staining according to our previous studies [11,12]. Moreover, Immunohistochemical staining was performed as previously described [12] with the antibodies of TGF-β1 and Smad2/3 (Santa Cruz Biotechnology).

### 2.6. Determination of AST, ALT, TNF-α, IL-6, IL-1β and MDA

Serum was instantly prepared and AST, ALT, TNF-α, IL-6 and IL-1β were detected using commercially available kits according to the manufacturer's instructions. Moreover, lipid peroxidation in the liver was assessed by detecting the content of malondialdehyde (MDA) as previously described [13].

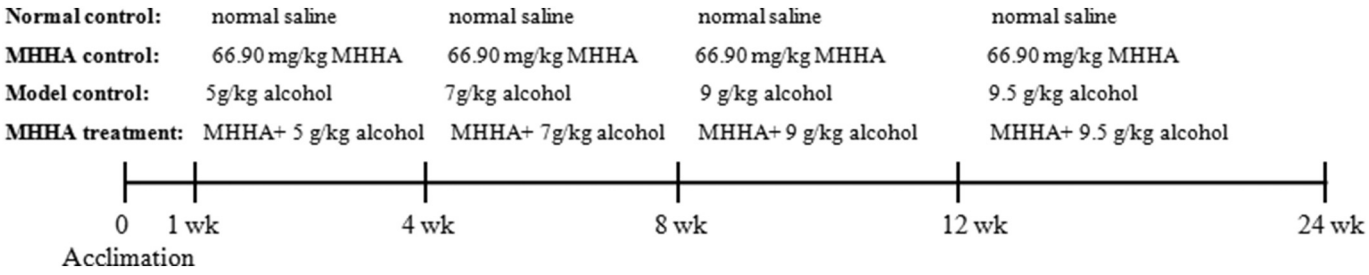


**Fig. 2.** The treatment schedule.

### 2.7. Determination of the collagen-related factors

Serum laminin (LN), hyaluronic acid (HA) and type III precollagen (PCIII), as well as hepatic hydroxyproline (HYP), were detected using commercially available kits according to the manufacturer's instructions as previously described [14].

### 2.8. Cell culture and cytotoxicity test

Human hepatic stellate cell line LX-2 was obtained from Shanghai MEIXUAN Biological science and technology LTD (Shanghai, China). Cells were cultured in RPMI Medium 1640 basic (1640, Hyclone) with 10% fetal bovine serum (FBS, Hyclone) and 100 IU/mL penicillin-streptomycin (Hyclone) at 37 °C in a humidified air containing 5% $CO_2$. The culture medium was changed every day.

To assess the cytotoxic effect of MHHA on HSCs, LX-2 cells were seeded in 96-well plates ($5 \times 10^3$ cells/well) and treated with MHHA at various concentration (3.125, 6.25, 12.5, 25, 50 or 100 μmol/L, MHHA was dissolved with 1% DMSO) or the same volume of DMSO (control cells) overnight and then each well was added 10 μL MTT (5 mg/mL) and incubated at 37 °C for 4 h. The absorbance was read at 490 nm using a microplate reader (Bio-Tek, USA). The half inhibitory concentration ($IC_{50}$) value was calculated. Survival (%) = $(1 - OD_{durg} / OD_{control}) \times 100\%$.

### 2.9. Determination of lactate dehydrogenase (LDH)

LX-2 cells were seeded in 6-well plates ($1 \times 10^6$ cells per well) for 24 h, and then treated with 10 ng/mL TGF-β1, followed by LY364947 (50 μmol/L) or MHHA (3, 6, or 12 μmol/L) for further 24 h. A normal control was also set. LDH was detected using the commercially available kit (Nanjing Jiancheng Bioengineering Institute, Nanjing, China) as previously described [15].

### 2.10. Acridine Orange/Ethylamine bromide (AO/EB) fluorescent staining

AO and EB are DNA intercalators (nucleic acid-specific fluorochromes), which emit a green and orange fluorescence, respectively, when bound to DNA [16]. Dual AO/EB fluorescent staining, visualized under a fluorescent microscope, can be used to identify apoptosis-associated changes of cell membranes during the process of apoptosis [17]. In this study, cell apoptosis was firstly evaluated by dual AO/EB staining as previously described [2]. LX-2 cells were plated in 6-well plates for 24 h and sequentially incubated with the various drugs as described above overnight. Cells were washed twice using PBS and treated with 10 μL AO/EB staining solution. Cells were observed and photographed with a fluorescence microscope.

### 2.11. Assessment of cell apoptosis

Cell apoptosis was also assessed by flow cytometry as previously described [14]. LX-2 cells were seeded in 6-well plates at a density of $1 \times 10^5$ cells/well overnight; and cells were then treated with the various drugs as described above for further 24 h. The cells were washed twice using PBS and centrifuged at 2000 rpm. Cells were re-suspended with 500 μL of annexin. Cell apoptosis was then assessed using the Annexin-V-FITC Apoptosis Detection Kit (Bestbio, Shanghai China) according to the manufacturer's instruction.

### 2.12. Flow cytometry for cell cycle analysis

LX-2 cells were seeded in 6-well plates at a density of $3 \times 10^5$ cells/well for 24 h and administrated with various drugs as described above for 24 h. The cells were washed twice with PBS, trypsinized and centrifuged at 2000 rpm for 5 min. For fixation, 500 μL ice-cold 70% ethanol was added to the cells for 4 h at 4 °C. Next, cells were washed and centrifuged at 800 rpm for 5 min. The cell pellet was resuspended in 100 μL RNase and incubated at 37 °C for 30 min. Then, cells were stained with 400 μL PI solution for 30 min in the dark at 4 °C. Cell cycle distribution was analyzed by flow cytometer using CellQuest software (BD Biosciences, CA, USA) as previously described [18].

### 2.13. Assessment of caspase-3 and caspase-9 activities

Following MHHA treatment as described above, LX-2 cells were washed twice with cold PBS. Each well was added with lysis buffer and incubated on ice for 20 min. The lysate was centrifuged at 16, 000 rpm at 4 °C for 20 min. The protein concentration in the supernatant was detected using the BCA™ Protein Assay Kit (Pierce, Rockford, IL, USA). Then, the activities of caspase-3 and -9 were determined with Caspase Assay Kit (BioVision Research Products, CA, USA).

### 2.14. Determination of mitochondria membrane potential (MMP)

Mitochondrial function was assessed by measuring MMP [14]. Briefly, LX-2 cells were cultured in 6-well plates overnight and then treated with the various drugs as described above for further 24 h. Then MMP was determined using Rhodamine123 staining as previously described [19].

### 2.15. Transient transfection and reporter gene assay

LX-2 cells were transfected with Lipofectamine 2000 (Life Technologies) containing the SMAD luciferase reporter plasmid (Genomeditech Co., Shanghai, China) as previously described [20]. Briefly, semi-confluent LX-2 cells in 6-well plates were transiently transfected with FuGENE1 6 Transfection Reagent (Roche Diagnostics, Indianapolis, IN) according to the manufacturer's instructions. Transfection efficiency was normalized by co-transfection of Renilla luciferase reporter plasmid pRL-TK (Promega, WI, MA, USA). Twenty-four hours after the transfection, cells were treated with TGF-β1 or MHHA for 24 h. The Smad transcriptional activity was measured using a Dual-Glo® Luciferase Assay System (Promega, WI, MA, USA) with a microplate reader (BioTek, USA) according to the manufacturer's instructions.

**Table 1**
Primer for RT-PCR assay in this study.

| Genes | Forward primer (5′-3′) | Reverse primer (5′-3′) |
|---|---|---|
| Col-I | GACATGTTCAGCTTTGTGGACCTC | AGGGACCCTTAGGCCATTGTGTA |
| Col-III | TTTGGCACAGCAGTCCAATGTA | GACAGATCCCGAGTCGCAGA |
| Bcl-2 | CAC CCC TGG CAT CTT CTC CT | GTT GAC GCT CCC CAC ACACA |
| Bax | GAC ATG TTT TCT GAC GGC AA | CCC AAA GTA GGA GAG GAG GC |
| TGF-β1 | CATTGCTGTCCCGTGCAGA | AGGTAACGCCAGGAATTGTTGCTA |
| TβRI | CACACGTCAGTGCGGTGAGAG | AGAGGCCCACAAGAGTTTCAACA |
| TβRII | GCGATCTAACCTGTTGCCTGTG | GGGCCATGTATCTCGCTGTTC |
| Smad2 | TTACAGATCCATCGAACTCGGAGA | CACTTAGGCACTCGGCAAACAC |
| Smad3 | GCACAGCAAGTTCCCAGTGTGTA | TGACAACTGAAATGCTGATCCAAAG |
| cyclin D | CTG GCC ATG AAC TAC CTG GA | CCA GGA AAT CAT GTG CAA TC |
| cyclin E | TTC TCG GCT CGC TCC AGG AA | TGG AGG ATA GAT TTC CTC |
| CDK2 | AGA TTC TTC TGG GCT GCA AG | AGA TCC GGA AGA GTT GGT CA |
| GAPDH | GGCACAGTCAAGGCTGAGAATG | ATGGTGGTGAAGACGCCAGTA |

### 2.16. RT-PCR assay

Total RNA from tissues or cells was extracted using the commercially available kit (KeyGEN BioTECH, China). The RT-PCR assay was carried out according to our previous study [19]. The primers used in this experiment were shown in Table 1.

### 2.17. Western blotting analysis

Western blotting was carried out as described in our previous work [21]. Briefly, the total protein from liver tissue or cells was lysed with RIPA buffer (Thermo Fischer Scientific, Inc., Waltham, MA) containing a protease inhibitor cocktail (Sigma-Aldrich) and its concentration was detected with BCA Protein Assay Kit (Beyotime, Jiangsu, China). Proteins were separated on 15% SDS-PAGE and electrotransferred onto PVDF membranes (Millipore, USA). The membrane was then blotted at 4 °C overnight with the various primary antibodies: Col-I (1:500), Col-III (1:500), α-SMA (1:1000), Bcl-2 (1:1000), Bax (1:1000), cytochrome C (1:500), TGF-β1 (1:500), Smad2/3 (1:500), p-Smad2/3 (1:500) and GAPDH (1:1000) (Santa Cruz Biotechnology). After the membranes were washed with TBST three times, they were incubated with horseradish peroxidase-labeled secondary antibody at room temperature for 1 h. The protein bands were washed with TBST and then detected using an ECL Western blotting kit.

### 2.18. Statistical analysis

Differences among all groups were analyzed by one-way analysis of variance, followed by SNK-q-test using SPSS10 software. $P < 0.05$ was accepted as statistically significant.

## 3. Results

### 3.1. MHHA ameliorated alcohol-induced liver injury

To assess histological changes, H&E staining of liver tissue sections from each group was examined. As shown in Fig. 3A, liver tissue from the normal control and MHHA control groups showed an intact lobular structure with clear central veins and radiating hepatic cords, without necrosis and inflammation (Fig. 3A1 and A2). On the contrary, the typical pathological characters including hepatocyte edema, loosening, necrosis and destruction were observed in the model group (Fig. 3A3). Interestingly, treatment with MHHA significantly alleviated the deleterious effects induced by chronic alcohol, as evidenced by the orderly hepatic cord, the clear lobule structure and the diminished necrosis (Fig. 3A4 to A6). Moreover, as shown in Fig. 3B, alcohol administration led to a significant increase in the activity of ALT and AST, however, MHHA treatment significantly decreased the activity of both the enzymes. These results suggested that MHHA significantly ameliorates alcohol-induced liver injury.

### 3.2. MHHA reduced collagen accumulation

Masson's trichrome staining showed that the liver tissue in the normal and MHHA control groups showed traces of collagen only in the walls of major blood vessels (Fig. 4A1 and A2). Chronic alcohol administration caused extensive accumulation of collagen (Fig. 4A3), while treatment with MHHA significantly decreased collagen deposition (Fig. 4A4 to A6). Similarly, Sirius red staining showed that red collagen fiber hyperplasia could be observed in the portal area in the model group, which was extended into the surrounding liver lobule to form thickly mixed fiber interval. However, red collagen fiber was significantly reduced in the MHHA-treated group (Fig. 4B). Moreover, the levels of HA, LN, PC III and HYP were strikingly increased in the model control group, while treatment with MHHA attenuated these biomarkers of liver fibrogenesis (Fig. 4C). Besides, treatment with MHHA significantly decreased the expression of collagen I and III, as evidenced by the results of RT-PCR assay and Western blotting (Fig. 4D and E). These results demonstrated that MHHA could inhibit collagen production and accumulation, alleviating hepatic fibrosis.

### 3.3. MHHA alleviated inflammation and lipid peroxidation

Compared to the normal control group, higher content of IL-6, IL-1β and TNF-α was observed in the model group. However, the abnormal levels of these inflammatory cytokines induced by alcohol were significantly alleviated by MHHA treatment (Fig. 5A). Moreover, the result indicated that the content of hepatic MDA increased dramatically in the model group, while treatment with MHHA effectively decreased its content (Fig. 5B).

### 3.4. Effects of MHHA on metabolic enzymes activity

The activity of ADH and ALDH in the model control group was significantly decreased, while treatment with MHHA significantly increased the activity of both of the enzymes (Fig. 6A). CYP2E1, one of the key metabolic enzymes in liver, plays a key role in the metabolism of alcohol [22]. As shown in Fig. 6B, chronic alcohol administration caused a significant increase in the activity of CYP2E1, but MHHA treatment had little effect on this enzyme.

### 3.5. MHHA inhibited HSC activation

As shown in Fig. 7A, cell viability was markedly inhibited by MHHA in a distinct dose-dependent manner. The IC50 of MHHA was 14.17 μmol/L. Moreover, as shown in Fig. 7B, treatment with MHHA significantly increased LDH activity, suggesting that MHHA can destroy cell membrane integrity. In addition, the result of Western blot showed

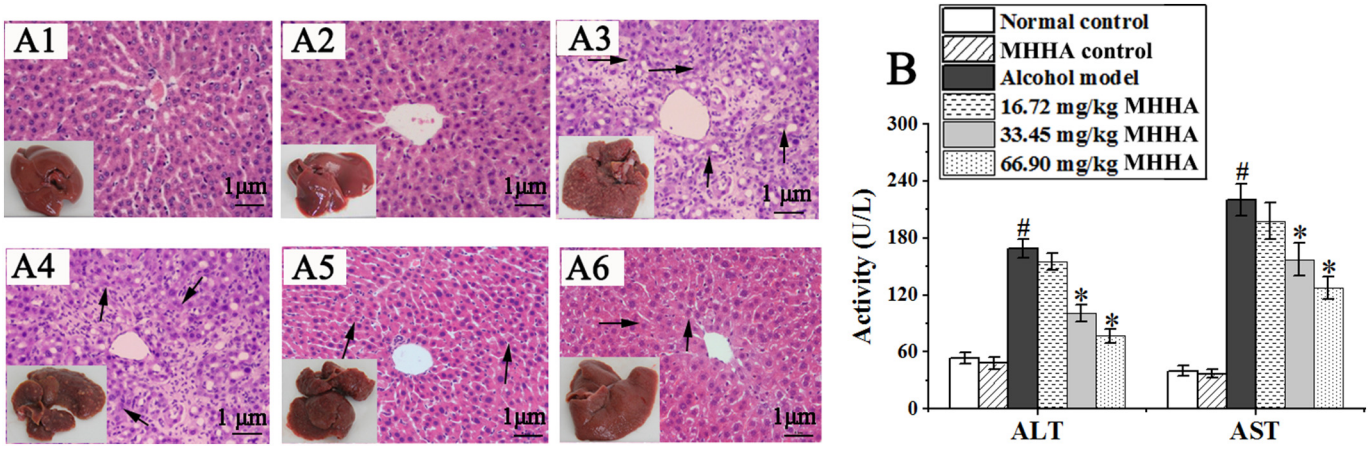


**Fig. 3.** MHHA ameliorated alcohol-induced liver injury. (A) Histological changes were observed using H&E staining (200×); A1: normal control, A2: MHHA control, A3: alcohol-model group, A4-A6: MHHA-treated groups (16.72, 33.45 and 66.90 mg/kg). The arrow indicates necrosis. (B) Serum alanine transaminase (ALT) and aspartate transaminase (AST) were measured using the commercially available kits. $^{\#}P < 0.05$ VS. normal control group and $^{*}P < 0.05$ VS. model group.

that α-SMA expression in LY364947 and MHHA-treated groups was notably decreased (Fig. 7C), suggesting that MHHA can inhibit HSC activation.

### 3.6. MHHA induced HSC apoptosis

As shown in Fig. 8A, AO/EB staining showed that TGF-β1 stimulation did not induce LX-2 cell apoptosis, whereas treatment with MHHA significantly induced cell apoptosis. Similarly, the result of the flow cytometry assay showed that MHHA treatment significantly increased the apoptosis ratio in a concentration-dependent manner (Fig. 8B). In addition, as shown in Fig. 8C and D, TGF-β1 stimulation did not showed significant effect on Bcl-2 and Bax expression both in mRNA and protein. However, LY364947 or MHHA treatment markedly increased Bax expression, but decreased Bcl-2 expression.

### 3.7. MHHA enhanced caspase-3 and -9 activities

As shown in Fig. 8E, TGF-β1 administration had little effect on the activities of caspase-3 and -9. LY364947 and MHHA treatment resulted in a significant dose-dependent increase in caspase-3 and -9 activities.

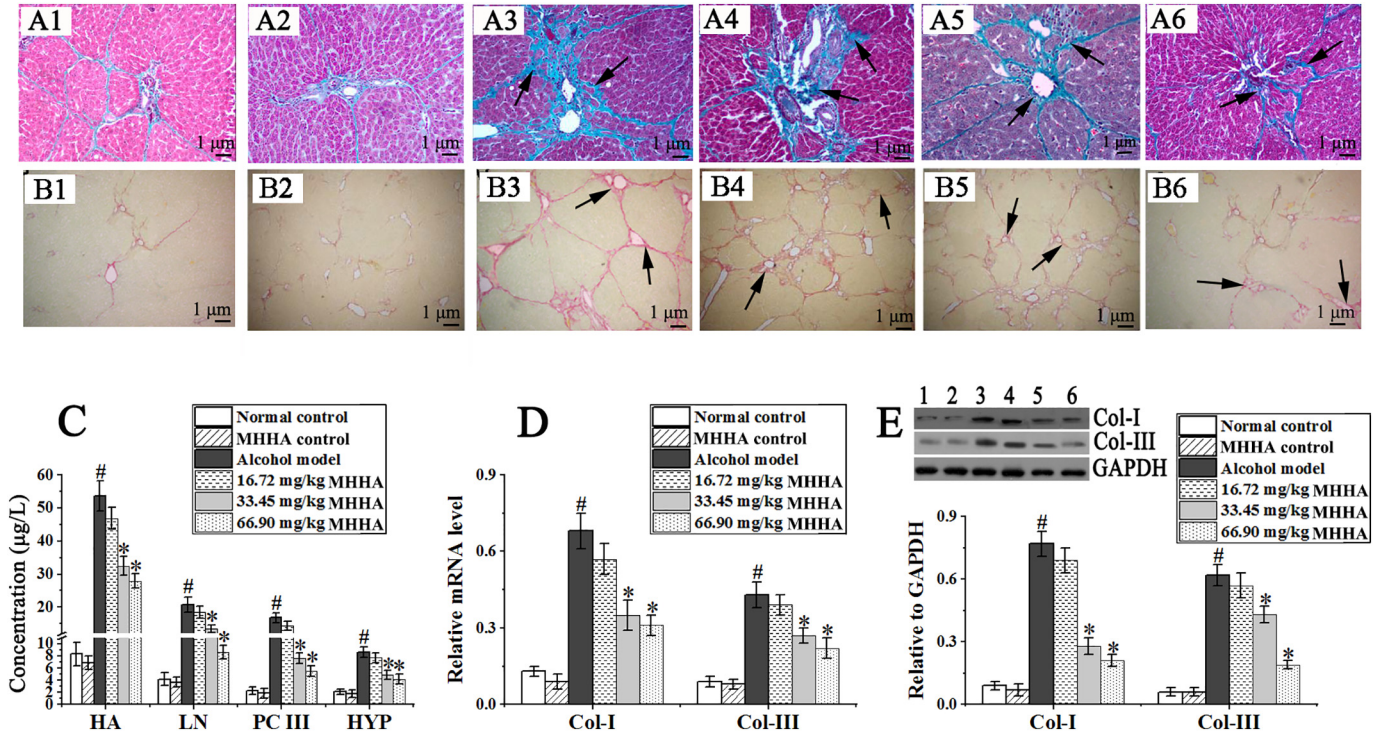


**Fig. 4.** MHHA reduced alcohol-induced collagen production. (A) and (B) Collagen deposition was assessed using Masson's trichrome and Sirius red staining (200×); The arrow means collagen deposition. A1 or B1: the normal control group; A2 or B2: the MHHA control group; A3 or B3: the alcohol model group; A4-A6 or B4-B5: the MHHA-treated groups (16.72, 33.45 and 66.90 mg/kg). (C) Serum HA, LN and PC III, and hepatic HYP were measured by commercial kits. (D) The gene expressions of collagen I and III were detected using RT-PCR assay. (E) The protein expressions of collagen I and III were detected by Western blotting. $^{\#}P < 0.05$ VS. normal control group and $^{*}P < 0.05$ VS. model group.

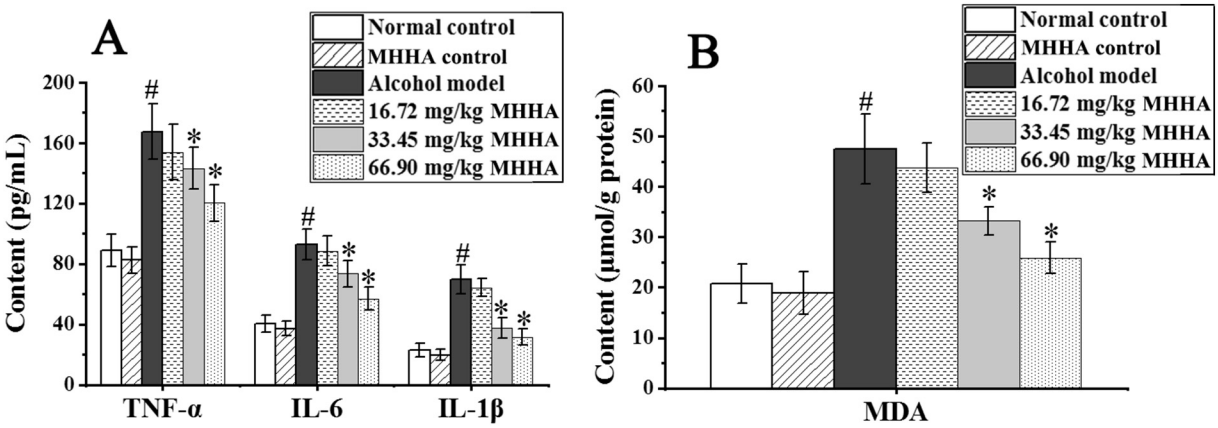


**Fig. 5.** MHHA alleviated alcohol-induced inflammatory response and lipid peroxidation. (A) Serum IL-6 , IL-1β and TNF-α were assayed with commercially available kits. (B) Hepatic MDA was measured using commercially available kit. $^{\#}P < 0.05$ VS. normal control group and $^{*}P < 0.05$ VS. model group.

### 3.8. MHHA induced cell cycle arrest at G2 phase

The analysis of flow cytometry showed that treatment with MHHA (12 μmol/L) significantly increased the accumulation of cells in G2 phase (Fig. 9A), suggesting that MHHA induced cell cycle arrest at G2 phase. To expose the underlying mechanism of MHHA on the cell cycle, the cell cycle-related genes were further detected. The results showed that treatment with MHHA notably decreased the transcription of cycle-related genes including cyclin D, cyclin E and CDK2, as assessed by RT-PCR analysis (Fig. 9B).

### 3.9. MHHA caused mitochondrial dysfunction

As shown in Fig. 10A, treatment with LY364947 and MHHA decreased MMP in a concentration-dependent manner, suggesting the possibility of MHHA to induce mitochondrial dysfunction. Furthermore, MHHA treatment decreased cytochrome *c* level in the mitochondria with a corresponding increase in cytosolic level, indicating that cytochrome *c* was released from the mitochondria to the cytosol (Fig. 10B). These findings suggest that mitochondrial dysfunction is likely involved in MHHA induced apoptosis. TGF-β1 administration had little effect on mitochondrial function.

### 3.10. MHHA inhibited the TGF-β1/Smads pathway

As shown in Fig. 11A and B, the Immunohistochemical staining showed that alcohol administration resulted in a significant increase in the expression of TGF-β1 and Smad2/3, while MHHA treatment markedly decreased their expression in a dose-dependent manner in rats. Similarly, the further experiment showed that MHHA treatment not only inhibited mRNA levels of TGF-β1, TβRI, TβRII, Smad2 and Smad3 in liver tissues (Fig. 11C), but also markedly reduced the content of TGF-β1 and TβRI/II protein and the phosphorylation of Smad2/3 both in liver tissues and LX-2 cells (Fig. 11D to E). Moreover, luciferase assay showed that MHHA treatment resulted in a significant decrease in Smad-luciferase activity, indicating that MHHA inhibits the Smad transcriptional activity in LX-2 cells (Fig. 11F). Taken together, these results suggest that MHHA treatment significantly inhibits the TGF-β1/Smad2/3 signaling pathway.

## 4. Discussion

In this study, hepatic fibrosis model was induced by alcohol in rats. Pathological examination demonstrated that chronic alcohol exposure caused serious changes to hepatic architecture; however, MHHA treatment significantly attenuated the degree of liver injury. Moreover, the serological assay revealed a significant increase in the activity of serum ALT and AST in the model group, indicating hepatocellular injury; while MHHA treatment notably decreased both the enzyme's activity. Furthermore, chronic alcohol administration caused extensive accumulation of collagen as indicated by the Masson's trichrome and Sirius red staining; and it also notably increased the contents of the collagen-related indicators, such as HA, LN, PCIII and HYP; however, these abnormal changes of collagen induced by alcohol were significantly reversed by MHHA treatment. These results suggest that MHHA treatment markedly ameliorates alcohol-induced hepatic injury

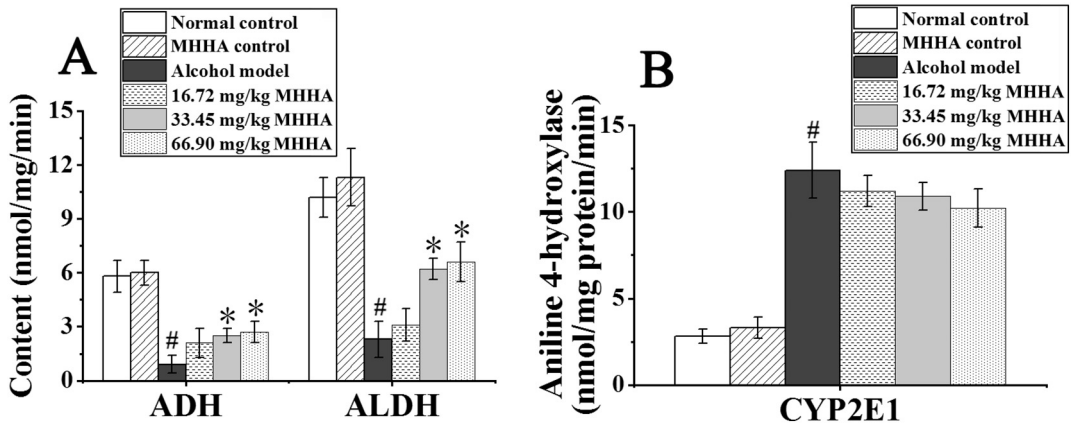


**Fig. 6.** The effects of MHHA on metabolic enzymes ADH, ALDH and CYP2E1. (A) ADH and ALDH were measured using commercially available diagnostic kits. (B) CYP2E1 was assessed by detecting the content of aniline 4-hydroxylase. $^{\#}P < 0.05$ VS. normal control group and $^{*}P < 0.05$ VS. model group.

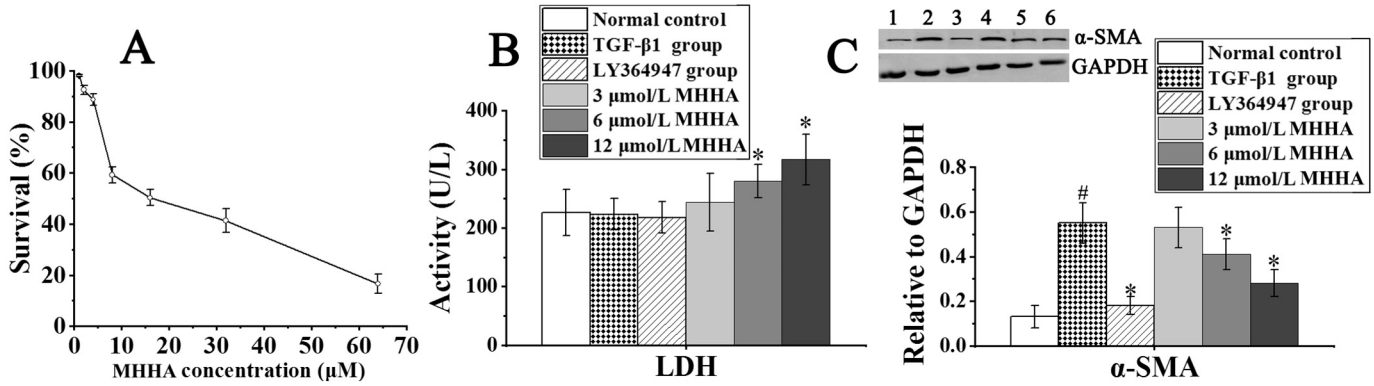


**Fig. 7.** MHHA inhibited HSC proliferation and activation. (A) Cytotoxicity of MHHA on LX-2 cells was determined by MTT assay. (B) Lactate dehydrogenase (LDH) was detected using a commercially available kit. (C) Protein expression of α-SMA was determined with Western blot assay. Band 1–6 represented the normal group, TGF-β1 group, LY364947 group, and MHHA treatment groups (3, 6 and 12 μmol/L). $^{\#}P < 0.05$ VS. normal control cells and $^{*}P < 0.05$ VS. TGF-β1 group.

and fibrosis in rats.

Generally, alcohol is oxidized to acetaldehyde by ADH enzyme. Subsequently, acetaldehyde enters the mitochondria where it is converted to acetate by ALDH [23]. Moreover, alcohol is also oxidized by CYP2E1, an alcohol-inducible isoform of CYP-450 enzymes [24]. In the present study, MHHA treatment significantly enhanced the activity of ADH and ALDH, but it had little effect on the activity of CYP2E1. These results suggest that MHHA increases the activity of metabolic enzymes, promoting alcohol metabolism and ultimately protecting hepatocytes from alcohol-induced injury. In addition, oxidative stress caused by alcohol metabolism is a major factor to induce liver injury [25]. MDA, a major end-product of lipid peroxidation, is commonly used as a biomarker for the assessment of radical-mediated oxidative stress. In the present study, MHHA treatment significantly attenuated alcohol-induced MDA activity as well as the expression of TNF-α, IL-6 and IL-1β, suggesting that the protection of MHHA against alcohol-induced liver injury might also be associated with the inhibition of lipid peroxidation and inflammatory mediator release.

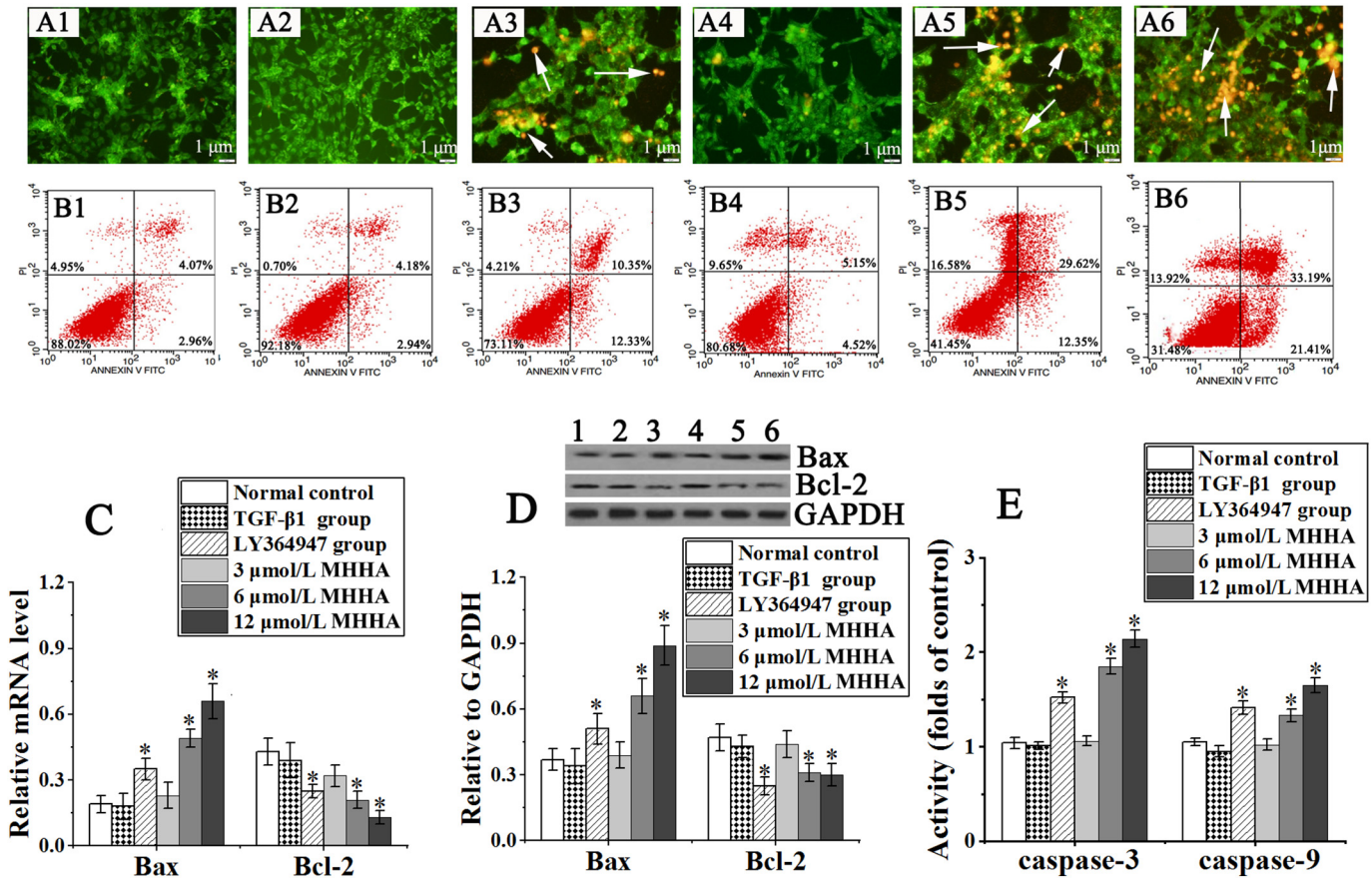


**Fig. 8.** MHHA significantly induced HSC apoptosis. (A-B) Cell apoptosis was assessed by AO/EB staining (200×) and flow cytometry, respectively; the arrow indicates hepatocyte apoptosis. A1 to A6 (or B1 to B6) represented the normal group, TGF-β1 group, LY364947 group, and MHHA treatment groups (3, 6 and 12 μmol/L), respectively. (C–D) Apoptosis-related genes and proteins were detected by using RT-PCR and Western blotting assays, respectively. Band 1–6 represented the normal group, TGF-β1 group, LY364947 group, and MHHA treatment groups (3, 6 and 12 μmol/L), respectively. (E) The activity of caspase-3 and -9 was determined by caspase-activity detection kits. $^{*}P < 0.05$ VS. TGF-β1 group and $^{\#}P < 0.05$ VS. normal control cells.

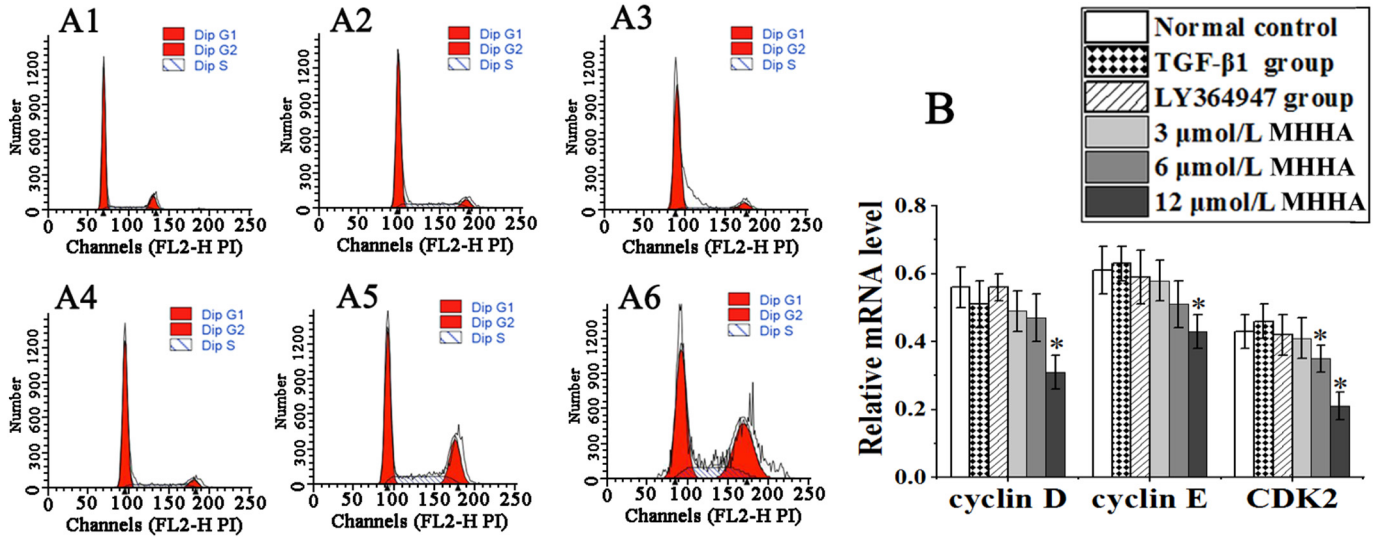


**Fig. 9.** MHHA induced cell cycle arrest at G2 phase. (A) Cell cycle was analyzed using flow cytometry; A1–A6 represented the normal group, TGF-β1 group, LY364947 group, and MHHA treatment groups (3, 6 and 12 μmol/L), respectively. (B) Cycle-related genes including cyclin D, cyclin E and CDK2 were detected by RT-PCR assay. $^{*}P < 0.05$ VS. TGF-β1 group.

HSCs, the major cellular source of the intrahepatic ECM, play an important role in hepatic fibrosis development [26]. In this study, MHHA treatment significantly inhibited LX-2 cell proliferation in a dose-dependent manner. Moreover, TGF-β1 stimulation significantly increased α-SMA expression; however treatment with MHHA notably reversed this change. These data suggest that MHHA can significantly inhibit HSC activation. To further confirm the cytotoxic effect of MHHA on HSCs, we also detected the level of LDH. We found that LDH was significantly increased after the cell was exposed to MHHA, suggesting that MHHA has a significant toxic effect on hepatic stellate cells. Additionally, the effect of MHHA on cell cycle was also analyzed. Our result showed that MHHA arrested cell cycle in the G2 phase, thus inhibiting the proliferation of HSCs. In summary, these results indicate that MHHA has a significant inhibitory effect on HSC proliferation and activation.

Apoptosis plays an important role in cell proliferation, differentiation, senescence and death. The potential to induce HSCs apoptosis has become an important strategy for the treatment of liver fibrosis [27]. In the present study, the result showed that MHHA markedly promoted LX-2 cell apoptosis. To further expose the mechanism of MHHA on cell apoptosis, the apoptosis-related proteins (Bcl-2 and Bax), caspases activity (caspases-3 and -9), and mitochondria membrane potential (MMP) were also assessed. It has been confirmed that apoptosis occurs through two primary pathways: the intrinsic pathway (the mitochondria-dependent pathway) and the extrinsic pathway that is associated with cell death receptors and their ligands on the cellular surface; and the former is the predominant apoptosis-inducing pathway [28]. The mitochondria-dependent apoptotic pathway is regulated by Bcl-2 family, including Bax and Bcl-2 [29]. Bax induces the opening of the mitochondrial permeability transition pore (MPTP), causing the release of cytochrome *c* from mitochondria to cytosol, whereas Bcl-2 inhibits the formation of the MPTP, reducing cytochrome *c* release [30]. An increase in the Bax/Bcl-2 ratio has been demonstrated to promote apoptosis by directly activating the mitochondrial apoptotic pathway [31]. Additionally, mitochondrial cytochrome *c* release is a key event in the activation of caspase-3 and -9, the downstream pivotal step to initiate apoptosis [32]. In the present study, we found that MHHA significantly increased the ratio of Bax/Bcl-2, enhanced the activity of caspases-3 and -9, and destroyed the function of mitochondria, suggesting that MHHA significantly induces LX-2 cell apoptosis likely via

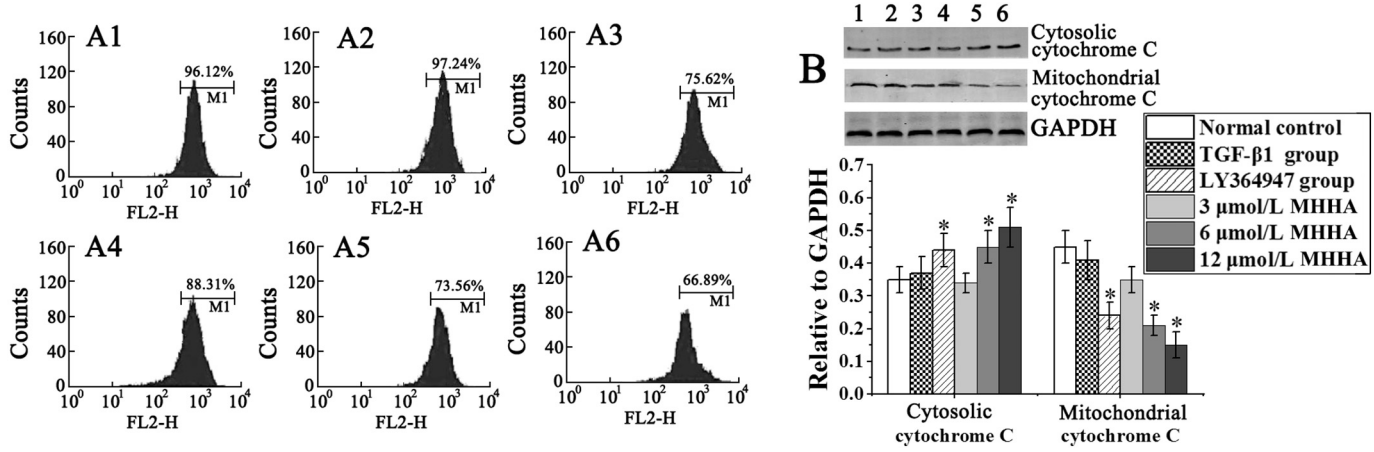


**Fig. 10.** MHHA induced mitochondrial dysfunction. (A) Mitochondria membrane potential (MMP) was analyzed by Rhodamine123 staining; A1 to A6 represented the normal group, TGF-β1 group, LY364947 group, and MHHA treatment groups (3, 6 and 12 μmol/L), respectively. (B) Cytochrome C was determined using Western blotting. Band 1–6 represented the normal group, TGF-β1 group, LY364947 group, and MHHA treatment groups (3, 6 and 12 μmol/L), respectively. $^{*}P < 0.05$ VS. TGF-β1 group.

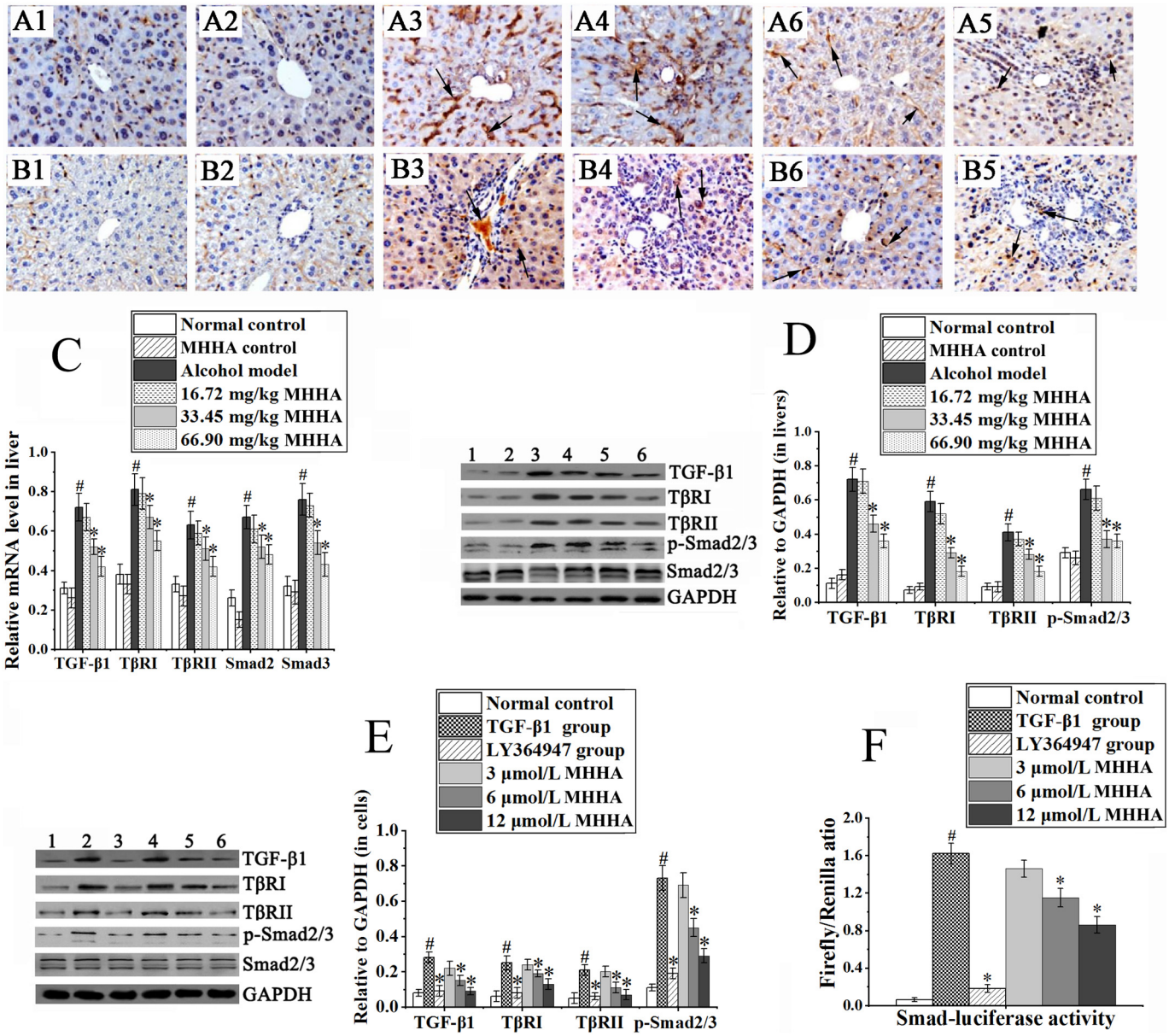


**Fig. 11.** MHHA blocked the TGF-β1/Smads pathway. (A) and (B) The expression of TGF-β1 and Smad2/3 was observed by Immunohistochemical staining. The expression of TGF-β1 and Smad2/3 was marked with brown staining as the arrow pointed. The expression of TGF-β1was mainly found in the ECM, while Smad2/3 was observed both in cytoplasm and nucleus. A1–A6 (or B1–B6) represented the normal group, TGF-β1 group, LY364947 group, and MHHA treatment groups (3, 6 and 12 μmol/L), respectively. (C) mRNA levels of TGF-β1, TβRI, TβRII, Smad2 and Smad3 in liver tissues were analyzed by RT-PCR. (D) TGF-β1and TβRI/II protein content and Smad2/3 phosphorylation in liver tissues were measured using Western blotting. (E) Protein expression of TGF-β1, TβRI and TβRII and the phosphorylation of Smad2/3 in LX-2 cells were detected by Western blotting. (F) The Smad transcriptional activity was measured using a Dual-Glo® Luciferase Assay System. In the animal experiment, $^{*}P < 0.05$ VS. model group and $^{\#}P < 0.05$ VS. normal control group; and in the cell experiment, $^{*}P < 0.05$ VS. TGF-β1 group and $^{\#}P < 0.05$ VS. normal control cells. (For interpretation of the references to color in this figure legend, the reader is referred to the web version of this article.)

modulation of the mitochondria-dependent pathway.

In the process of liver fibrosis, TGF-β1 is one of the most potent fibrogenesis factors with certain effect on promoting ECM by activating HSCs [5]. Once activated, TGF-β binds to the membrane receptor, promoting the phosphorylations of Smad2/3. Afterwards, a heteromeric complex is formed by the phosphorylated Smad2/3 and Smad4, which can transfer into the nucleus and activate the transcription of profibrotic genes [5]. In this study, we found that TGF-β1 stimulation significantly increased collagen accumulation, promoted HSC proliferation and activation, and decreased HSC apoptosis; on the other hand LY364947 (a TGF-β1 receptor inhibitor) notably abolished these effects of TGF-β1 on LX-2 cells. Interestingly, treatment with MHHA significantly inhibited the expressions of TGF-β1, TβRI, TβRII and the phosphorylation of Smad2/3 in liver tissues and LX-2 cells. Moreover, luciferase assay showed that MHHA treatment led to a significant decrease in Smad-luciferase activity. These results suggest that MHHA ameliorates liver fibrosis maybe through inhibiting the TGF-β1/Smad2/3 pathway.

In summary, our study demonstrates that MHHA can alleviate alcohol-induced liver fibrosis and the underlying mechanism may be ascribed to the inhibition of the TGF-β1/Smads pathway and regulation of the mitochondria-mediated apoptotic pathway (Fig. 12). MHHA may be developed as a potential medicine for the treatment of liver fibrosis in the future.

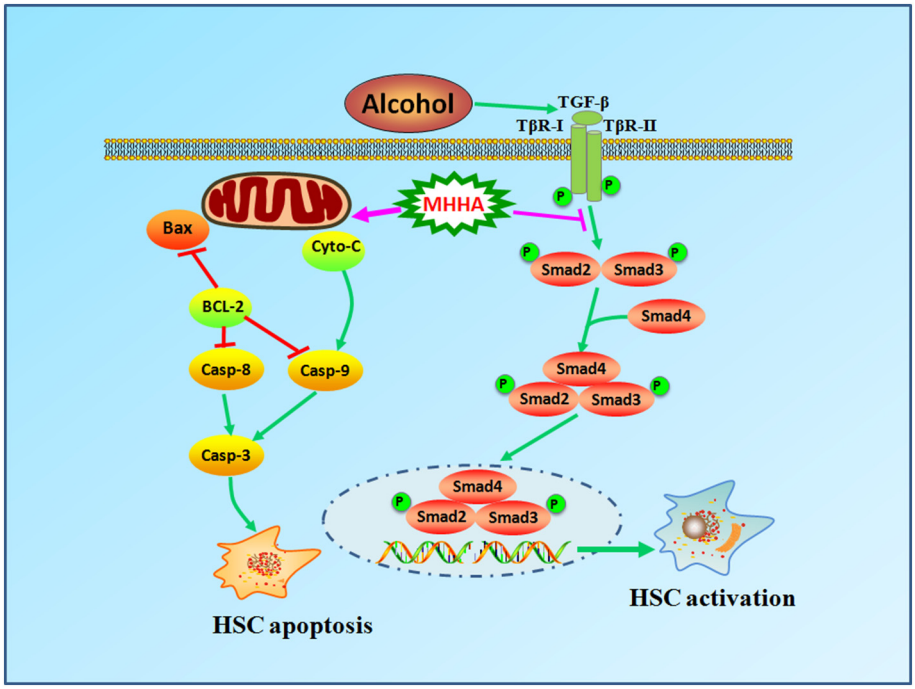


**Fig. 12.** MHHA significantly reduced HSC activation by inhibiting the TGF-β1/Smads signaling pathway and notably induced HSC apoptosis by modulating the mitochondria-mediated apoptotic pathway. MHHA decreased the phosphorylations of Smad2/3 and then inhibited the heteromeric complex formed by p-Smad2/3 and Smad4 to transfer into cell nucleus, which down-regulated the transcription of profibrotic genes and therefore inhibited HSC activation. Moreover, MHHA increased the ratio of Bax/Bcl-2 and sequentially led to mitochondrial dysfunction, cytochrome C release and caspase abnormal increase, finally inducing HSC apoptosis.

## Declaration of Competing Interest

The authors declare that there are no conflicts of interest.

## Acknowledgments

The authors gratefully acknowledge the financial support provided by the Guangxi Natural Science Foundation (2016GXNSFDA380025), the National Natural Science Foundation of China (No. 81660693; No. 81660686; No. 81873087) and the Innovation Project of Guangxi Graduate Education (YCBZ2019038).

## References

[1] Q. Huang, C. Liang, L. Wei, J. Nie, S. Lu, C. Lu, et al., Raf kinase inhibitory protein down-expression exacerbates hepatic fibrosis in vivo and in vitro, Cell. Physiol. Biochem. 40 (2016) 49–61.
[2] K. Liu, P.C. Liu, R. Liu, X. Wu, Dual AO/EB staining to detect apoptosis in osteosarcoma cells compared with flow cytometry, Med. Sci. Monit. Basic Res. 21 (2015) 15–20.
[3] T. Kisseleva, D.A. Brenner, Role of hepatic stellate cells in fibrogenesis and the reversal of fibrosis, J. Gastroenterol. Hepatol. 22 (Suppl. 1) (2007) S73–S78.
[4] C. Liu, X. Chen, L. Yang, T. Kisseleva, D.A. Brenner, E. Seki, Transcriptional repression of the transforming growth factor β (TGF-β) pseudoreceptor BMP and activin membrane-bound inhibitor (BAMBI) by nuclear factor κB (NF-κB) p50 enhances TGF-β signaling in hepatic stellate cells, J. Biol. Chem. 289 (2014) 7082–7091.
[5] F. Xu, C. Liu, D. Zhou, L. Zhang, TGF-β/SMAD pathway and its regulation in hepatic fibrosis, J. Histochem. Cytochem. 64 (2016) 157–167.
[6] D. Schuppan, Y.O. Kim, Evolving therapies for liver fibrosis, J. Clin. Invest. 123 (2013) 1887–1901.
[7] Q. Huang, Y. Li, S. Zhang, R. Huang, L. Zheng, L. Wei, et al., Effect and mechanism of methyl helicterate isolated from Helicteres angustifolia (Sterculiaceae) on hepatic fibrosis induced by carbon tetrachloride in rats, J. Ethnopharmacol. 143 (2012) 889–895.
[8] Q.F. Huang, S.J. Zhang, L. Zheng, M. Liao, M. He, R. Huang, et al., Protective effect of isoorientin-2″-O-α-L-arabinopyranosyl isolated from Gypsophila elegans on alcohol induced hepatic fibrosis in rats, Food Chem. Toxicol. 50 (2012) 1992–2001.
[9] X.-H. Zhang, M. Yan, L. Liu, T.-J. Wu, L.-L. Ma, L.-X. Wang, Expression of discoidin domain receptors (DDR2) in alcoholic liver fibrosis in rats, Arch. Med. Res. 41 (2010) 586–592.
[10] X. Lin, R. Huang, S. Zhang, L. Zheng, L. Wei, M. He, et al., Methyl helicterate protects against CCl4-induced liver injury in rats by inhibiting oxidative stress, NF-kappaB activation, Fas/FasL pathway and cytochrome P4502E1 level, Food Chem. Toxicol. 50 (2012) 3413–3420.
[11] Q. Huang, R. Huang, S. Zhang, J. Lin, L. Wei, M. He, et al., Protective effect of genistein isolated from Hydrocotyle sibthorpioides on hepatic injury and fibrosis induced by chronic alcohol in rats, Toxicol. Lett. 217 (2013) 102–110.
[12] Q. Wang, X. Dai, W. Yang, H. Wang, H. Zhao, F. Yang, et al., Caffeine protects against alcohol-induced liver fibrosis by dampening the cAMP/PKA/CREB pathway in rat hepatic stellate cells, Int. Immunopharmacol. 25 (2015) 340–352.
[13] M.E. Shaker, H.A. Salem, G.E. Shiha, T.M. Ibrahim, Nilotinib counteracts thioacetamide-induced hepatic oxidative stress and attenuates liver fibrosis progression, Fundam. Clin. Pharmacol. 25 (2011) 248–257.
[14] F. Bai, Q. Huang, J. Nie, S. Lu, C. Lu, X. Zhu, et al., Trolline ameliorates liver fibrosis by inhibiting the NF-κB pathway, promoting HSC apoptosis and suppressing autophagy, Cell. Physiol. Biochem. 44 (2017) 436–446.
[15] T. Larsen, Determination of lactate dehydrogenase (LDH) activity in milk by a fluorometric assay, J. Dairy Res. 72 (2005) 209–216.
[16] N. Atale, S. Gupta, U. Yadav, V. Rani, Cell-death assessment by fluorescent and non-fluorescent cytosolic and nuclear staining techniques, J. Microsc. 255 (2014) 7–19.
[17] S. Miao, X. Mao, R. Pei, S. Miao, et al., Lepista sordida polysaccharide induces apoptosis of Hep-2 cancer cells via mitochondrial pathway, Int. J. Biol Macromol. 61 (2013) 97–101.
[18] P. Pozarowski, Z. Darzynkiewicz, Analysis of cell cycle by flow cytometry, Methods Mol. Biol. 281 (2004) 301–311.
[19] X. Lin, J. Wei, Y. Chen, P. He, J. Lin, S. Tan, et al., Isoorientin from Gypsophila elegans induces apoptosis in liver cancer cells via mitochondrial-mediated pathway, J. Ethnopharmacol. 187 (2016) 187–194.
[20] S. Quan, W. Yan, Z. Jie, L. Jing, ENMD-1068 inhibits liver fibrosis through attenuation of TGF-β1/Smad2/3 signaling in mice, Sci. Rep. 7 (2017) 5498.
[21] L. Xing, F. Bai, J. Nie, S. Lu, C. Lu, X. Zhu, et al., Didymin alleviates hepatic fibrosis through inhibiting ERK and PI3K/Akt pathways via regulation of Raf kinase inhibitor protein, Cell. Physiol. Biochem. 40 (2016) 1422–1432.
[22] I. Kessova, A.I. Cederbaum, CYP2E1: biochemistry, toxicology, regulation and function in ethanol-induced liver injury, Curr. Mol. Med. 3 (2003) 509–518.
[23] C.K. Sung, S.M. Kim, C.J. Oh, S.A. Yang, B.H. Han, E.K. Mo, Taraxerone enhances alcohol oxidation via increases of alcohol dehyderogenase (ADH) and acetaldehyde dehydrogenase (ALDH) activities and gene expressions, Food Chem. Toxicol. 50 (2012) 2508–2514.
[24] Y. Lu, A. Cederbaum, CYP2E1 and oxidative liver injury by alcohol, Free Radic. Biol. Med. 44 (2008) 723–738.
[25] M. Tamura, H. Matsui, T. Kaneko, I. Hyodo, Alcohol is an oxidative stressor for gastric epithelial cells: detection of superoxide in living cells, J. Clin. Biochem. Nutr. 53 (2013) 75–80.
[26] A.I. Serban, L. Stanca, O.I. Geicu, M.C. Munteanu, A. Dinischiotu, RAGE and TGF-β1 cross-talk regulate extracellular matrix turnover and cytokine synthesis in AGEs exposed fibroblast cells, PLoS One 11 (2016) e0152376.
[27] S. Jin, H. Li, M. Han, M. Ruan, Z. Liu, F. Zhang, et al., Mesenchymal stem cells with enhanced Bcl-2 expression promote liver recovery in a rat model of hepatic cirrhosis, Cell. Physiol. Biochem. 40 (2016) 1117–1128.
[28] S. Fulda, K.M. Debatin, Extrinsic versus intrinsic apoptosis pathways in anticancer chemotherapy, Oncogene 25 (2006) 4798–4811.
[29] D. Kong, T. Zheng, M. Zhang, D. Wang, S. Du, X. Li, et al., Static mechanical stress induces apoptosis in rat endplate chondrocytes through MAPK and mitochondria-dependent caspase activation signaling pathways, PLoS One 8 (2013) e69403.
[30] Y. Wang, X. Li, X. Wang, W. Lau, Y. Wang, Y. Xing, et al., Ginsenoside Rd attenuates myocardial ischemia/reperfusion injury via Akt/GSK-3beta signaling and inhibition of the mitochondria-dependent apoptotic pathway, PLoS One 8 (2013) e70956.
[31] J.K. Brunelle, A. Letai, Control of mitochondrial apoptosis by the Bcl-2 family, J. Cell Sci. 122 (2009) 437–441.
[32] D. Green, G. Kroemer, The central executioners of apoptosis: caspases or mitochondria? Trends Cell Biol. 8 (1998) 267–271.